Rab35 regulates Arf6 activity through centaurin-β2 (ACAP2) during neurite outgrowth

Hotaka Kobayashi and Mitsunori Fukuda*

Laboratory of Membrane Trafficking Mechanisms, Department of Developmental Biology and Neurosciences, Graduate School of Life Sciences, Tohoku University, Aobayama, Aoba-ku, Sendai, Miyagi 980-8578, Japan

*Author for correspondence (nori@m.tohoku.ac.jp)

Accepted 10 January 2012
Journal of Cell Science 125, 2235–2243

doi: 10.1242/jcs.098657

Summary

Two small GTPases, Rab and Arf, are well-known molecular switches that function in diverse membrane-trafficking routes in a coordinated manner; however, very little is known about the direct crosstalk between Rab and Arf. Although Rab35 and Arf6 were independently reported to regulate the same cellular events, including endocytic recycling, phagocytosis, cytokinesis and neurite outgrowth, the molecular basis that links them remains largely unknown. Here we show that centaurin-β2 (also known as ACAP2) functions both as a Rab35 effector and as an Arf6-GTPase-activating protein (GAP) during neurite outgrowth of PC12 cells. We found that Rab35 accumulates at Arf6-positive endosomes in response to nerve growth factor (NGF) stimulation and that centaurin-β2 is recruited to the same compartment in a Rab35-dependent manner. We further showed by knockdown and rescue experiments that after the Rab35-dependent recruitment of centaurin-β2, the Arf6-GAP activity of centaurin-β2 at the Arf6-positive endosomes was indispensable for NGF-induced neurite outgrowth. These findings suggest a novel mode of crosstalk between Rab and Arf: a Rab effector and Arf-GAP coupling mechanism, in which Arf-GAP is recruited to a specific membrane compartment by its Rab effector function.

Key words: Rab35, Centaurin-β2, ACAP2, Arf6, Membrane traffic, Neurite outgrowth

Introduction

Rab-type and Arf-type small GTPases function as molecular switches that drive or stop membrane trafficking by cycling between a GTP-bound active state (ON state) and a GDP-bound inactive state (OFF state) (reviewed by Zerial and McBride, 2001; D'Souza-Schorey and Chavrier, 2006; Fukuda, 2008; Stenmark, 2009). GTP-bound active Rab and Arf drive membrane trafficking by recruiting a specific effector molecule to active Rab- or Arf-resident organelles or vesicles. The cycling is controlled by two regulatory factors, a guanine nucleotide exchange factor (GEF), which activates Rab and Arf, and a GTPase-activating protein (GAP), which inactivates them (Barr and Lambright, 2010). In mammals, the Rab family and Arf family consist of approximately 60 members and 30 members, respectively, and it has been suggested that they control highly diverse membrane-trafficking routes in a coordinated manner (Wennerberg et al., 2005). However, how the actions of these distinct types of small GTPases are functionally coordinated is poorly understood, because very little is known about the direct crosstalk between Rab and Arf.

Rab35 was originally reported to regulate the process of recycling internalized components back to the plasma membrane (i.e. endocytic recycling) (Kouranti et al., 2006; Patino-Lopez et al., 2008; Sato et al., 2008; Allaire et al., 2010), but it was later reported to also regulate neurite outgrowth, an essential process in the establishment of initial neural connectivity. Expression of a constitutive active Rab35 mutant was found to promote neurite outgrowth of PC12 cells and neuroblastoma N1E-115 cells (Chevallier et al., 2009; Kanno et al., 2010; Fukuda et al., 2011), although the exact mechanism of the Rab35-mediated neurite outgrowth remains to be elucidated. Involvement of the Arf-type small GTPase Arf6 in neurite outgrowth has also been reported (reviewed by Jaworski, 2007). In contrast to Rab35, however, expression of a constitutive active Arf6 mutant has been found to inhibit neurite outgrowth of rat hippocampal neurons (Hernández-Deviez et al., 2004). Although two small GTPases, Rab35 and Arf6, are likely to be involved in neurite outgrowth in a coordinated fashion, little is known about their functional relationships or whether Rab35 and Arf6 regulate neurite outgrowth independently, sequentially or cooperatively.

In this study, we analyzed the function of Arf6-GAP centaurin-β2 (also known as ACAP2) (Jackson et al., 2000), which has recently been reported to be an active Rab35-binding protein (Kanno et al., 2010). We showed that centaurin-β2 is recruited to Arf6-positive endosomes through a direct interaction with Rab35 and that centaurin-β2 inactivates Arf6 after its recruitment to the Arf6-positive endosomes during neurite outgrowth of PC12 cells. We discuss the novel crosstalk between Rab35 and Arf6 through centaurin-β2 suggested by our findings.

Results

Rab35 and centaurin-β2 are essential factors for neurite outgrowth

We and others have previously shown that expression of the constitutive active mutant of Rab35 [Rab35(Q67L)] in PC12 cells enhances NGF-induced neurite outgrowth, whereas its constitutive negative mutant [Rab35(S22N)] inhibits it (Chevallier et al., 2009; Kanno et al., 2010). However, the involvement of endogenous

Rab35 molecules in NGF-induced neurite outgrowth of PC12 cells has never been investigated. To do so, we first investigated endogenous expression of Rab35 in PC12 cells by immunoblotting with a Rab35-specific antibody (Fig. 1C, lane 1, top panel) and evaluated the effect on neurite outgrowth of Rab35 knockdown with specific siRNAs (Fig. 1C, lanes 2 and 3 in the top panel). As expected, the results showed a dramatic reduction in the total neurite length of Rab35-depleted PC12 cells, in comparison with the control cells (Fig. 1A,B). The same result – strong inhibition of NGF-induced neurite outgrowth – was obtained when a Rab35-specific GAP, TBC1D10C (EPI64C) (Patino-Lopez et al., 2008; Hsu et al., 2010), was overexpressed in PC12 cells (data not shown). These findings indicated that endogenous Rab35 is actually an essential mediator of neurite outgrowth of PC12 cells.

The first step in determining the molecular mechanism responsible for the Rab35-mediated neurite outgrowth of PC12 cells was to identify the downstream effector of Rab35. Although several Rab35-binding proteins have been reported in the literature (Fukuda et al., 2008; Zhang et al., 2009; Kanno et al., 2010), we focused on Arf6-GAP centaurin-β2 (ACAP2) (supplementary material Fig. S1) as a candidate Rab35 effector, because centaurin-β2 was found to bind GTP-Rab35 specifically among the 60 mammalian Rab proteins tested (Kanno et al., 2010) and it is endogenously expressed in PC12 cells (Fig. 1F, lane 1, top panel). If centaurin-β2 actually functions as a downstream effector of Rab35, centaurin-β2 should also be required for NGF-induced neurite outgrowth. To investigate this possibility, we knocked down endogenous centaurin-β2 molecules in PC12 cells with specific shRNAs (Fig. 1F) and evaluated their effect on neurite outgrowth. As shown in Fig. 1D,E, a dramatic reduction in the neurite length of centaurin-β2-depleted cells was observed (Fig. 1E), similar to the Rab35-depleted cells described above, suggesting that centaurin-β2 functions as a downstream effector of Rab35 in the neurite outgrowth of PC12 cells. Because depletion of either Rab35 or centaurin-β2 in cultured mouse hippocampal neurons also resulted in the same phenotype, i.e. a dramatic reduction in neurite length (supplementary material Fig. S2), Rab35 and centaurin-β2 also regulate the neurite outgrowth of neuronal cells.

Rab35 recruits centaurin-β2 to Arf6-positive endosomes during neurite outgrowth

Next, we produced and used specific antibodies against Rab35 and centaurin-β2 (supplementary material Fig. S3) to analyze the subcellular localization of endogenous Rab35 and centaurin-β2 in PC12 cells before and after NGF stimulation. Although previous overexpression studies indicated that exogenously expressed Rab35 is mainly localized at the plasma membrane and the intracellular compartments (Zhang et al., 2009; Kanno et al., 2010; Hsu et al., 2010), our confocal microscopic analyses revealed no clear Rab35 signals in unstimulated PC12 cells

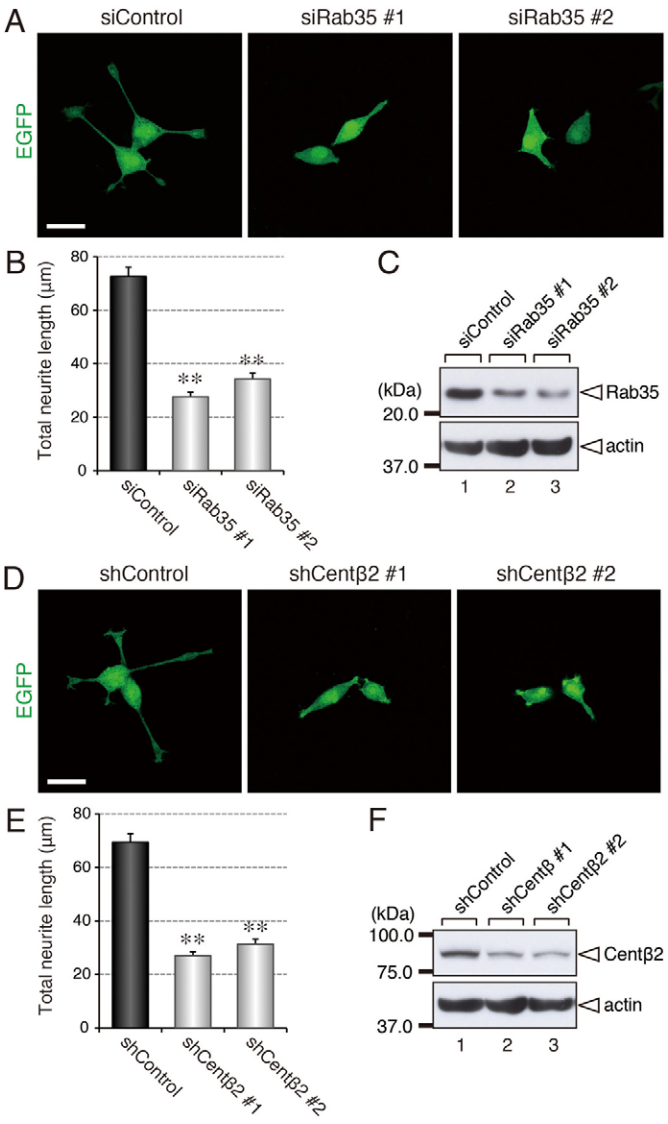

Fig. 1. Rab35 and centaurin-β2 are required for NGF-induced neurite outgrowth of PC12 cells. (**A**) Typical images of control siRNA (siControl)-treated and *Rab35* siRNA (siRab35)-treated PC12 cells after NGF stimulation for 36 hours. siRNA-treated cells were identified by the green fluorescence of EGFP. Scale bar: 30 μm. (**B**) Effect of Rab35 knockdown on neurite outgrowth of PC12 cells. Bars represent the total neurite length values (mean and s.e.) of siControl-treated (control; black bar), siRab35#1-treated (left white bar), and siRab35#2-treated (right white bar) cells ($n>100$). $^{**}P<0.01$, in comparison with the control cells (Student's unpaired *t*-test). Note that siRNA-mediated knockdown of Rab35 dramatically inhibited neurite outgrowth of PC12 cells. (**C**) Reduced expression of endogenous Rab35 in siRab35-treated PC12 cells. Cell lysates of PC12 cells treated with either siControl, siRab35#1 or siRab35#2 were subjected to 10% SDS-PAGE followed by immunoblotting with anti-Rab35 antibody (top panel; 1:500 dilution) and anti-actin antibody (bottom panel; 1:200 dilution). The positions of the molecular mass markers (in kDa) are shown on the left. (**D**) Typical images of control shRNA (shControl)-treated and *Centb2* shRNA (shCentβ2)-treated PC12 cells after NGF stimulation for 36 hours. shRNA-treated cells were identified by the green fluorescence of EGFP. Scale bar: 30 μm. (**E**) Effect of centaurin-β2-knockdown on neurite outgrowth of PC12 cells. Bars represent the total neurite length values (mean and s.e.) of shControl-treated (control; black bar), shCentβ2#1-treated (left white bar), and shCentβ2#2-treated (right white bar) cells ($n>100$). $^{**}P<0.01$, in comparison with the control cells (Student's unpaired *t*-test). Note that shRNA-mediated knockdown of centaurin-β2 dramatically inhibited neurite outgrowth of PC12 cells, the same as knockdown of Rab35 did. (**F**) Reduced expression of endogenous centaurin-β2 in shCentβ2-treated PC12 cells. Cell lysates of PC12 cells treated with either shControl, shCentβ2#1, or shCentβ2#2 were subjected to 10% SDS-PAGE followed by immunoblotting with anti-centaurin-β2 antibody (top panel; 1:200 dilution) and anti-actin antibody (bottom panel; 1:200 dilution). The positions of the molecular mass markers (in kDa) are shown on the left.

(Fig. 2A, NGF 0 hour; no NGF stimulation). To our surprise, however, rapid accumulation of Rab35 signals in the perinuclear area was observed in response to NGF stimulation (Fig. 2A, top row, NGF 1 hour and 6 hours). Interestingly, a similar change (i.e. accumulation in the perinuclear area) in the distribution of centaurin-β2 was observed (Fig. 2A, middle row, NGF 1 hour and 6 hours). Moreover, the centaurin-β2 signals closely colocalized with the Rab35 signals in the perinuclear area [Fig. 2A, bottom row, NGF 1 hour and 6 hours; Fig. 2B; Pearson's correlation coefficient (PCC), 0.85±0.04], suggesting that centaurin-β2 regulates neurite outgrowth in concert with Rab35. Such accumulation is likely to be attributable to the increased local concentration of Rab35 and centaurin-β2 in the perinuclear area in response to NGF stimulation, because their levels of expression before and after NGF stimulation were similar (Fig. 2C).

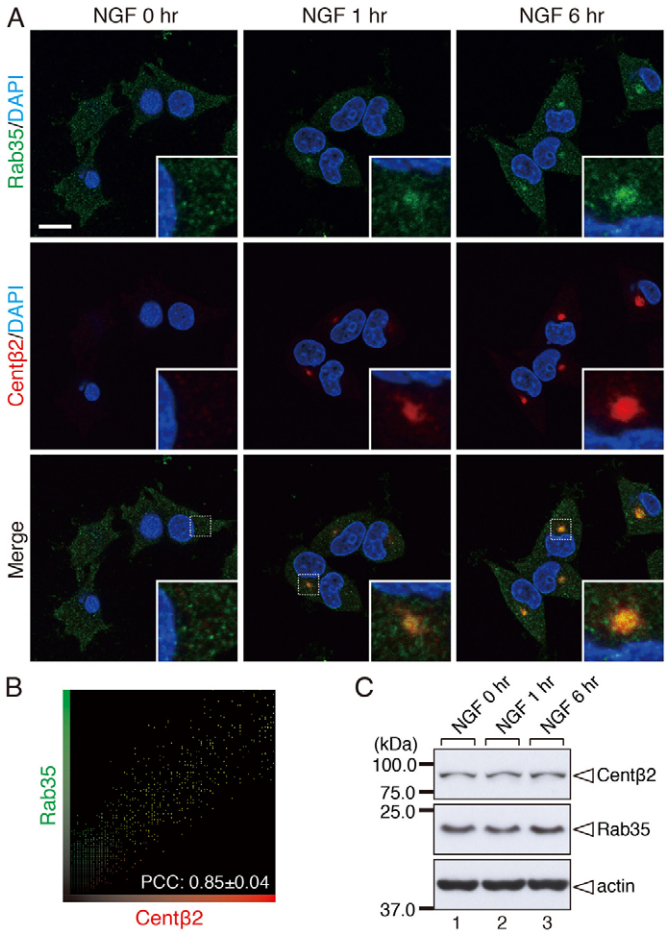

Fig. 2. Rab35 and centaurin-β2 accumulate to the perinuclear area of PC12 cells in an NGF-dependent manner. (**A**) Subcellular localization of endogenous Rab35 and centaurin-β2 (Centβ2) in PC12 cells in response to NGF stimulation. After NGF stimulation for 0 hour (no NGF treatment), 1 hour and 6 hours, PC12 cells were fixed, and then stained with anti-Rab35 antibody (green; 1:100 dilution), anti-centaurin-β2 antibody (red; 1:100 dilution) and DAPI (nuclei; blue). Note that both Rab35 and centaurin-β2 are recruited to the perinuclear area in an NGF-dependent manner. Scale bar: 10 μm. (**B**) Intensity scatterplot of Rab35 signals (green) and centaurin-β2 signals (red) in PC12 cells after NGF stimulation for 6 hours. The Pearson's correlation coefficient (PCC) (mean and s.d.) for the relation between them is shown at the bottom (n=30 from three independent experiments). (**C**) Unaltered expression of endogenous Rab35 and centaurin-β2 in PC12 cells during NGF stimulation. After NGF stimulation for 0 hour, 1 hour and 6 hours, cell lysates of PC12 cells were subjected to 10% SDS-PAGE followed by immunoblotting with anti-Rab35 antibody (middle panel; 1:500 dilution), anti-centaurin-β2 antibody (top panel; 1:200 dilution), and anti-actin antibody (bottom panel; 1:200 dilution). The positions of the molecular mass markers (in kDa) are shown on the left.

The colocalization of Rab35 and centaurin-β2 in the perinuclear area in NGF-stimulated PC12 cells led us to hypothesize that centaurin-β2 is recruited to Rab35-positive perinuclear regions through a direct interaction with Rab35. We tested our hypothesis by investigating the subcellular localization of centaurin-β2 in Rab35-depleted PC12 cells in the presence of NGF stimulation. The results showed that the centaurin-β2 signals were significantly reduced in Rab35-depleted PC12 cells (Fig. 3A,B), indicating that Rab35 is required for the perinuclear recruitment of centaurin-β2. By contrast, knockdown of centaurin-β2 had no significant effect on the perinuclear localization and expression of Rab35 (Fig. 3C,D,F). Because the level of expression of centaurin-β2 was unaltered by Rab35 knockdown (Fig. 3E), centaurin-β2 is likely to be dispersed from Rab35-positive perinuclear compartments into the cytosol (or other membrane compartments) in Rab35-depleted PC12 cells.

To identify the perinuclear compartment in which centaurin-β2 was recruited by Rab35, we co-stained for Rab35, centaurin-β2 and several organelle markers, including EEA-1 (an early endosome marker), GM130 (a Golgi marker), Rab7 (a late endosome and lysosome marker), Rab11 (a recycling endosome marker) and γ-tubulin (a centrosome marker), and quantitatively analyzed their colocalization using PCC (supplementary material Fig. S4). The results of the immunofluorescence analysis indicated that endogenous Rab35 and centaurin-β2 were present at the pericentrosomal area and that they partially colocalized with Rab11 (data not shown; supplementary material Fig. S4A,B; PCC, 0.31±0.14). Because Arf6, a target of centaurin-β2, has been shown to be localized at recycling endosomes (Donaldson, 2003; van Ijzendoorn, 2006), we next investigated the subcellular localization of endogenous Arf6 in PC12 cells by immunocytochemistry. The results showed that Arf6 closely colocalized with endogenous Rab35 and centaurin-β2 in the pericentrosomal area in NGF-stimulated PC12 cells (Fig. 4A,B, arrowheads; Fig. 4C,D; PCCs, 0.67±0.08 and 0.72±0.06, respectively). Judging from the PCC values, neither Rab35 nor centaurin-β2 colocalized with any of the other organelle markers (data not shown; supplementary material Fig. S4C; –0.20<PCCs<0.20) (however, limited colocalization with EEA-1 was observed at a few punctate structures; supplementary material Fig. S3A, arrowhead). We therefore concluded that Rab35 and centaurin-β2 were mainly localized at pericentrosomal Arf6-positive endosomes.

The Arf6-GAP activity of centaurin-β2 is required for neurite outgrowth

Because centaurin-β2 has been reported as an Arf6-GAP and Arf6 has been suggested to be involved in neurite outgrowth of neuronal cells (Albertinazzi et al., 2003; Hernández-Deviez et al., 2004; Yamauchi et al., 2009), we investigated the possible involvement of crosstalk between Rab35 and Arf6 through centaurin-β2 during neurite outgrowth. To do so, we first attempted to determine the significance of the Rab35-dependent recruitment of centaurin-β2 to Arf6-positive endosomes by using a knockdown and rescue

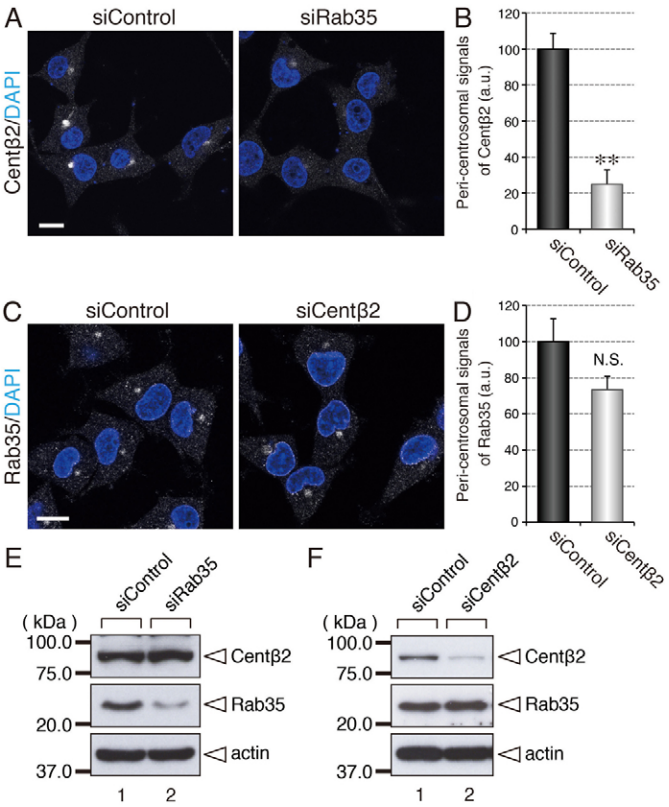

Fig. 3. Rab35 recruits centaurin-β2 to the perinuclear area of PC12 cells. (**A**) Subcellular localization of endogenous centaurin-β2 in Rab35-depleted PC12 cells after NGF stimulation for 6 hours. PC12 cells transfected with control siRNA (siControl) or *Rab35* siRNA (siRab35) were fixed and stained with anti-centaurin-β2 antibody (white; 1:100 dilution) and DAPI (nuclei; blue). Scale bar: 10 μm. (**B**) Effect of Rab35 knockdown on pericentrosomal localization of centaurin-β2. Bars represent the pericentrosomal centaurin-β2 signals (mean and s.e.; arbitrary units, a.u.) of siControl-treated (control; black bar) and siRab35-treated (white bar) cells ($n=30$ from three independent experiments). $^{**}P<0.01$, in comparison with control cells (Student's unpaired *t*-test). Note that the pericentrosomal centaurin-β2 signals were significantly decreased in Rab35-depleted cells. (**C**) Subcellular localization of endogenous Rab35 in centaurin-β2-depleted PC12 cells after NGF stimulation for 6 hours. PC12 cells transfected with control siRNA (siControl) or *Centb2* siRNA (siCentβ2) were fixed, and then stained with anti-Rab35 antibody (white; 1:100 dilution) and DAPI (nuclei; blue). Scale bar: 10 μm. (**D**) Effect of centaurin-β2 knockdown on pericentrosomal localization of Rab35. Bars represent the pericentrosomal Rab35 signals (mean and s.e.; arbitrary units, a.u.) of siControl-treated (control; black bar) and siCentβ2-treated (white bar) cells ($n=30$ from three independent experiments). N.S., not significant in comparison with the control cells. Note that knockdown of centaurin-β2 had no significant effect on the Rab35 signals in the pericentrosomal area. (**E**) Unaltered expression of endogenous centaurin-β2 in Rab35-depleted PC12 cells compared with control cells. Cell lysates of PC12 cells treated with either siControl or siRab35 were subjected to 10% SDS-PAGE followed by immunoblotting with anti-centaurin-β2 antibody (top panel; 1:200 dilution), anti-Rab35 antibody (middle panel; 1:500 dilution), and anti-actin antibody (bottom panel; 1:200 dilution). The positions of the molecular mass markers (in kDa) are shown on the left. (**F**) Unaltered expression of endogenous Rab35 in centaurin-β2-depleted PC12 cells when compared with control cells. Cell lysates of PC12 cells treated with either siControl or siCentβ2 were subjected to 10% SDS-PAGE followed by immunoblotting as described in E.

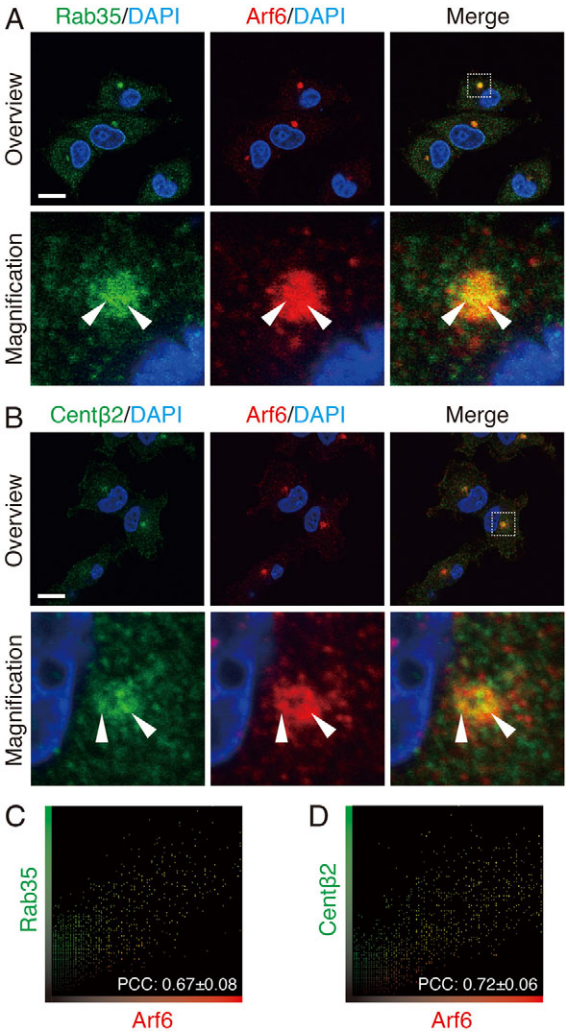

Fig. 4. Rab35 and centaurin-β2 colocalize with Arf6. (**A**) Subcellular localization of endogenous Rab35 and Arf6 after NGF stimulation for 6 hours. NGF-stimulated PC12 cells were fixed, and then stained with anti-Rab35 antibody (green; 1:100 dilution), anti-Arf6 antibody (red; 1:100 dilution), and DAPI (nuclei; blue). Note that Rab35 and Arf6 are colocalized in the perinuclear area (arrowheads). Scale bar: 10 μm. The arrowheads indicate colocalization between Rab35 and Arf6. (**B**) Subcellular localization of endogenous centaurin-β2 (Centβ2) and Arf6 after NGF stimulation. After NGF stimulation for 6 hours PC12 cells were fixed, and then stained with anti-centaurin-β2 antibody (green; 1:100 dilution), anti-Arf6 antibody (red; 1:100 dilution) and DAPI (nuclei; blue). Note that centaurin-β2 and Arf6 are colocalized in the perinuclear area (arrowheads). Scale bar: 10 μm. The lower panels in A and B are magnified views of the boxed areas in the upper right panels. The arrowheads indicate colocalization between centaurin-β2 and Arf6. (**C**) Intensity scatterplot of Rab35 signals (green) and Arf6 signals (red) in PC12 cells after NGF stimulation for 6 hours. The Pearson's correlation coefficient (PCC) (mean and s.d.) for the relation between them is shown at the bottom ($n=30$ from three independent experiments). (**D**) Intensity scatterplot of centaurin-β2 signals (green) and Arf6 signals (red) in PC12 cells after NGF stimulation for 6 hours. The PCC (mean and s.d.) for the relation between them is shown at the bottom ($n=30$ from three independent experiments).

approach, and a Rab35-binding-deficient mutant of centaurin-β2 named ΔANKR, which lacks the Rab35-binding ankyrin repeat domain (ANKR) but contains an intact Arf6-GAP domain (supplementary material Fig. S1) (Kanno et al., 2010).

Consistent with the above finding that centaurin-β2 is recruited to Arf6-positive endosomes in a Rab35-dependent manner, Myc-tagged centaurin-β2(ΔANKR) dramatically reduced its ability to localize at the Arf6-positive endosomes in NGF-stimulated PC12 cells (Fig. 5A, middle row). More importantly, re-expression of an shRNA-resistant (SR) mutant of centaurin-β2(ΔANKR)^{SR} (supplementary material Fig. S5B) in centaurin-β2-depleted PC12 cells did not rescue the inhibitory effect of *Centb2* shRNA on NGF-induced neurite outgrowth, whereas re-expression of the wild-type centaurin-β2^{SR} (supplementary material Fig. S5A) restored neurite outgrowth (Fig. 5B,C). These results allowed us to conclude that Rab35-dependent recruitment of centaurin-β2 to Arf6-positive endosomes is required for NGF-induced neurite outgrowth to occur.

To confirm that centaurin-β2 inactivates Arf6 after its recruitment to the pericentrosomal endosomes during NGF-induced neurite outgrowth, we used an Arf6-GAP activity-deficient mutant of centaurin-β2 named RQ, in which arginine residue 442 of centaurin-β2 is replaced by glutamine (supplementary material Fig. S1) (Jackson et al., 2000). Although the centaurin-β2(RQ) mutant was able to target Arf6-positive pericentrosomal endosomes (Fig. 5A, bottom row) through the ANKR domain, to a similar level as the wild-type protein, re-expression of the centaurin-β2(RQ)^{SR} (supplementary material Fig. S5C) in centaurin-β2-depleted PC12 cells did not rescue the inhibitory effect of *Centb2* shRNA on NGF-induced neurite outgrowth (Fig. 5D,E), indicating that inactivation of Arf6 at the pericentrosomal endosomes by centaurin-β2 is essential for NGF-induced neurite outgrowth to occur. Consistent with this finding, overexpression of a constitutive active mutant of Arf6 [Arf6(Q67L)] in PC12 cells strongly inhibited NGF-induced neurite outgrowth (Fig. 6D).

Arf6 functions downstream of Rab35 during neurite outgrowth

Finally, we investigated whether Arf6 itself actually functions in the downstream of Rab35 during NGF-induced neurite outgrowth of PC12 cells. To do so, we knocked down endogenous Arf6 molecules in PC12 cells with specific siRNAs (supplementary material Fig. S6C, lanes 2 and 3 in top panel) and evaluated their effect on Rab35-mediated neurite outgrowth. Knockdown of endogenous Arf6 molecules by specific siRNAs caused a reduction in the neurite length of Arf6-depleted cells in comparison with the control cells (supplementary material Fig. S6A,B), a finding that was consistent with the previous report that Arf6 is required for neurite outgrowth of N1E-115 cells (Yamauchi et al., 2009). We noted that the same *Arf6* siRNAs suppressed the Rab35(Q67L)-dependent enhancement of neurite outgrowth to the level of neurite outgrowth by the control cells (Fig. 6A,C). Moreover, we found that overexpression of a constitutive active mutant of Arf6 [Arf6(Q67L)] in PC12 cells strongly inhibited NGF-induced neurite outgrowth (Fig. 6D) and

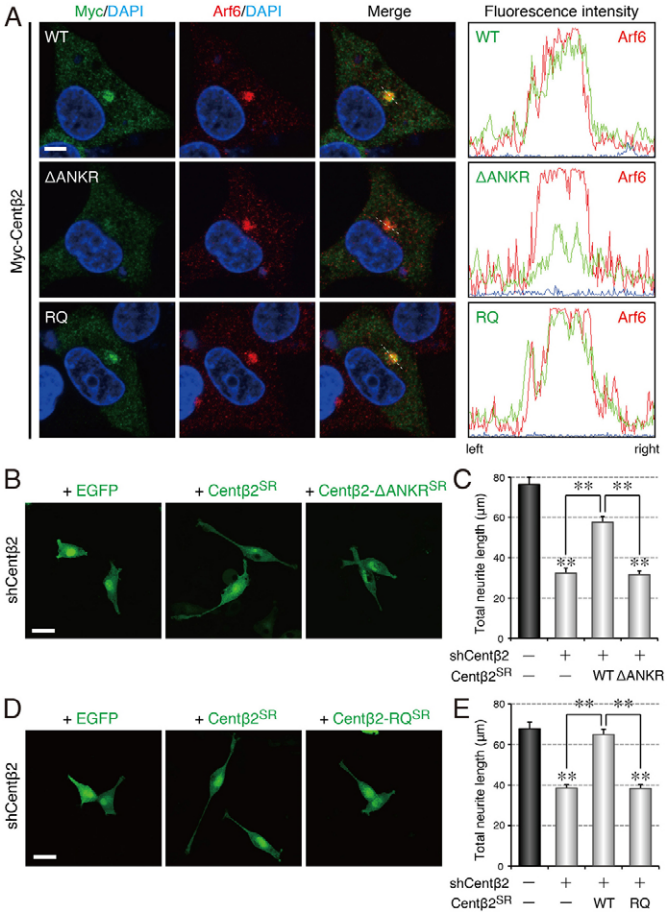

Fig. 5. Arf6-GAP activity of centaurin-β2 is required for NGF-induced neurite outgrowth of PC12 cells after Rab35-dependent recruitment. (**A**) Colocalization analysis of wild-type centaurin-β2 (Centβ2-WT), centaurin-β2(ΔANKR) (Centβ2-ΔANKR), and centaurin-β2(RQ) (Centβ2-RQ) with endogenous Arf6 in PC12 cells after NGF stimulation for 36 hours. PC12 cells transiently expressing either Myc-Centβ2(WT), Myc-Centβ2(ΔANKR), or Myc-Centβ2(RQ) (left panels) were fixed, and then stained with anti-Myc antibody (left panels; 1:500 dilution) and anti-Arf6 antibody (middle panels; 1:100 dilution). Merged images are shown in the right panels. Fluorescence intensity along white dashed lines (right panels) is shown on the right. Note that the Rab35-binding-deficient Centβ2(ΔANKR) mutant had impaired ability to localize at the Arf6-positive pericentrosomal compartment. Scale bar: 5 μm. (**B**) Typical images of EGFP–Centβ2(WT)^{SR}-expressing and EGFP–Centβ2(ΔANKR)^{SR}-expressing PC12 cells after NGF stimulation for 36 hours under centaurin-β2-depleted conditions. Scale bar: 30 μm. (**C**) Effect of EGFP–Centβ2(WT)^{SR} and EGFP–Centβ2(ΔANKR)^{SR} expression on neurite outgrowth under centaurin-β2-depleted conditions. Bars represent the total neurite length values (mean and s.e.) of control shRNA (shControl) + EGFP-expressing (control; black bar), *Centb2* shRNA (shCentβ2) + EGFP-expressing (left white bar), shCentβ2 + EGFP–Centβ2(WT)^{SR}-expressing (central white bar), and shCentβ2 + EGFP–Centβ2(ΔANKR)^{SR}-expressing (right white bar) cells (n>100). **P<0.01, in comparison with the control cells (Student's unpaired t-test). Note that the shRNA-resistant EGFP–Centβ2(ΔANKR)^{SR} mutant did not rescue the effect of centaurin-β2 knockdown on neurite outgrowth, whereas expression of EGFP–Centβ2(WT)^{SR} in centaurin-β2-depleted cells restored neurite outgrowth. (**D**) Typical images of EGFP–Centβ2(WT)^{SR}-expressing and EGFP–Centβ2(RQ)^{SR}-expressing PC12 cells after NGF stimulation for 36 hours under centaurin-β2-depleted conditions. Scale bar: 30 μm. (**E**) Effect of EGFP–Centβ2(WT)^{SR} and EGFP–Centβ2(RQ)^{SR} expression on neurite outgrowth under centaurin-β2-depleted conditions. Bars represent the total neurite length values (mean and s.e.) of shControl + EGFP-expressing (control; black bar), shCentβ2 + EGFP-expressing (left white bar), shCentβ2 + EGFP–Centβ2(WT)^{SR}-expressing (central white bar) and shCentβ2 + EGFP–Centβ2(RQ)^{SR}-expressing (right white bar) cells (n>100). **P<0.01, in comparison with the control cells (Student's unpaired t-test). Note that the shRNA-resistant EGFP–Centβ2(RQ)^{SR} mutant did not rescue the effect of centaurin-β2 knockdown on neurite outgrowth, whereas expression of EGFP–Centβ2(WT)^{SR} in centaurin-β2-depleted cells restored neurite outgrowth.

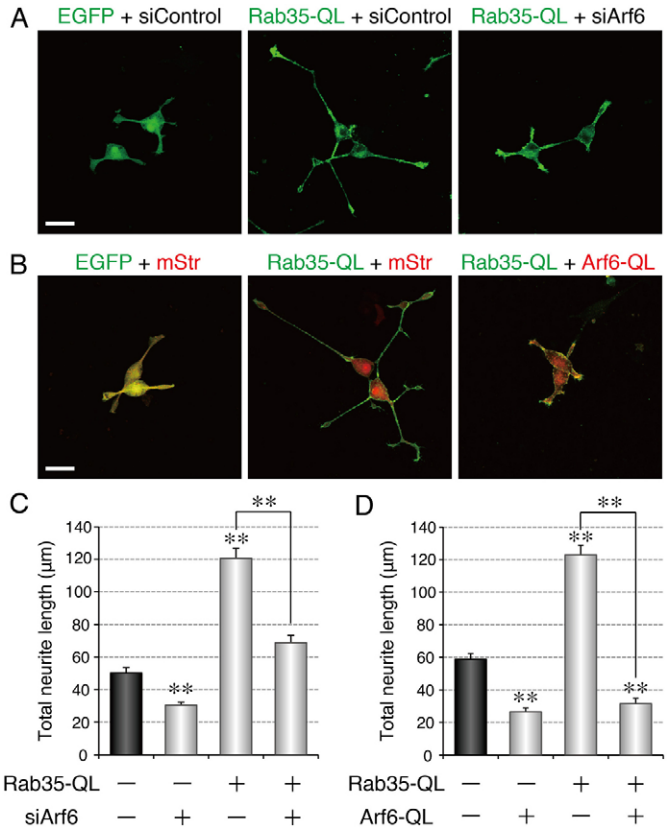

Fig. 6. Arf6 functions downstream of Rab35 in neurite outgrowth of PC12 cells. (**A**) Typical images of EGFP–Rab35(QL) + control siRNA (siControl)-expressing and EGFP–Rab35(QL) + *Arf6* siRNA (siArf6)-expressing PC12 cells after NGF stimulation for 36 hours. Scale bar: 30 μm. (**B**) Typical images of EGFP–Rab35(QL) + mStr-expressing and EGFP–Rab35–(QL) + Arf6(QL)–mStr-expressing PC12 cells after NGF stimulation for 36 hours. Scale bar: 30 μm. (**C**) Effect of Arf6 knockdown on active Rab35-promoted neurite outgrowth of PC12 cells. Bars represent the total neurite length values (mean and s.e.) of EGFP + siControl-expressing (control; black bar), EGFP + siArf6-expressing (left white bar), EGFP–Rab35(QL) + siControl-expressing (central white bar) and EGFP–Rab35(QL) + siArf6-expressing (right white bar) cells ($n>100$). $^{**}P<0.01$, in comparison with the control cells (Student's unpaired *t*-test). Note that Rab35(QL)-dependent promotion of neurite outgrowth was dramatically inhibited by knockdown of endogenous Arf6. (**D**) Effect of expression of Arf6(QL) on active Rab35-promoted neurite outgrowth of PC12 cells. Bars represent the total neurite length values (mean and s.e.) of EGFP + mStr-expressing (control; black bar), Arf6(QL)–mStr + EGFP-expressing (left white bar), mStr + EGFP–Rab35(QL)-expressing (central white bar) and Arf6(QL)–mStr + EGFP–Rab35(QL)-expressing (right white bar) cells ($n>100$). $^{**}P<0.01$, in comparison with the control cells (Student's unpaired *t*-test). Note that the Rab35(QL)-dependent promotion of neurite outgrowth was completely inhibited by co-expression with Arf6(QL).

that its co-expression with Rab35(Q67L) in PC12 cells strongly inhibited the Rab35(Q67L)-dependent enhancement of the neurite outgrowth (Fig. 6B,D). Taken together, these findings indicate that the inactivation of Arf6 downstream of Rab35 is required for NGF-induced neurite outgrowth of PC12 cells.

Discussion

Although Rab and Arf have been reported to function as key regulators of membrane trafficking (Zerial and McBride, 2001; D'Souza-Schorey and Chavrier, 2006; Stenmark, 2009), the functional crosstalk between these two small GTPases is poorly understood. One known link between Rab and Arf is a crosstalk between Rab11 and Arf6 mediated by Rab11-FIP3 (Arfophilin-1), which functions as a 'dual effector' for Rab11 and Arf6 (Fielding et al., 2005; Shiba et al., 2006; Schonteich et al., 2007). In the present study, we discovered a novel mode of crosstalk between Rab35 and Arf6 mediated by centaurin-β2, which functions as both a Rab35 effector and an Arf6-GAP (i.e. 'Rab effector and Arf-GAP coupling') during neurite outgrowth of PC12 cells. On the basis of the results of the knockdown and rescue experiments in combination with mutational analyses, we propose the following mechanism to explain the regulation of neurite outgrowth by Rab35 and Arf6 (Fig. 7): (1) Rab35 accumulates at Arf6-positive pericentrosomal endosomes in an NGF-dependent manner (Figs 2, 4); (2) centaurin-β2 is recruited to the same compartment through a direct interaction with Rab35 (Figs 3, 4); (3) the recruited centaurin-β2 inactivates pericentrosomal Arf6 during neurite outgrowth of PC12 cells (Fig. 5). Consistent with our proposal, expression of the constitutive active mutant of Rab35 [Rab35(Q67L)] has been reported to enhance neurite outgrowth of neuronal cells (Chevallier et al., 2009; Kanno et al., 2010), whereas expression of the constitutive active mutant of Arf6 [Arf6(Q67L)] has been reported to inhibit it (Hernández-Deviez et al., 2004).

Our findings that endogenous Rab35 and centaurin-β2 are localized mainly at the pericentrosomal Arf6-positive endosomes in PC12 cells (Fig. 4A,B; supplementary material Fig. S4A) are consistent with previous reports showing that exogenously expressed Rab35 colocalized with EHD1, which is known to be localized at recycling endosomes (Lin et al., 2001; Allaire et al., 2010), and that Arf6 was also localized at the same compartment (Donaldson, 2003; van Ijzendoorn, 2006). However, Rab35 has also been reported to localize at other intracellular compartments, e.g. the plasma membrane, in other cell types (Kouranti et al., 2006; Allaire et al., 2010). Such discrepancies might be

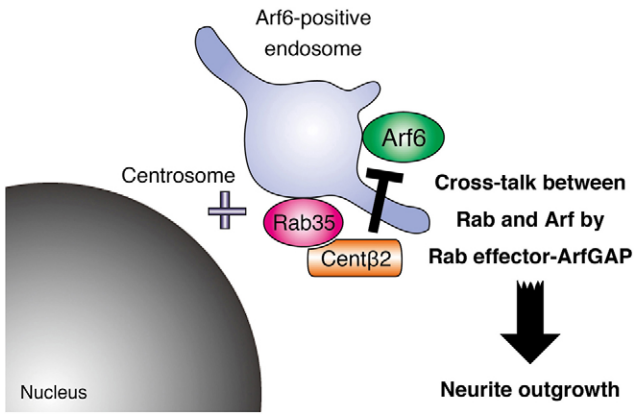

Fig. 7. A model of the crosstalk between Rab35 and Arf6 through centaurin-β2 during neurite outgrowth. Rab35 is recruited to the pericentrosomal Arf6-positive endosomes in response to NGF stimulation and recruits its effector, centaurin-β2, to the same compartment in PC12 cells (Figs 2–4). Centaurin-β2 then inactivates Arf6 at the pericentrosomal endosomes through its Arf6-GAP activity during neurite outgrowth (Fig. 5). Inactivation of Arf6 at the pericentrosomal endosomes is required for the Rab35-mediated neurite outgrowth (Figs 1,6).

attributable to differences in the experimental conditions (e.g. endogenous proteins versus exogenously expressed proteins) and/or the cell lines used. Actually, consistent with a previous report (Kouranti et al., 2006), we detected immunofluorescence signals of Rab35 at the plasma membrane of HeLa cells when we used our own antibody in the present study (data not shown), suggesting that localization of Rab35 varies somewhat according to the cell type. We also found that exogenously expressed Rab35 was clearly localized at the plasma membrane in PC12 cells (Fig. 6A,B) (Kanno et al., 2010), as well as at Arf6-positive endosomes (data not shown). Interestingly, however, hardly any endogenous centaurin-β2 was recruited to the plasma membrane in exogenously Rab35-expressing PC12 cells (data not shown), even though exogenously expressed centaurin-β2 was clearly targeted to the plasma membrane by exogenous Rab35 and artificially inhibited neurite outgrowth by inactivating Arf6 at the plasma membrane (Kanno et al., 2010). We therefore speculate that centaurin-β2 is specifically recruited to the Arf6-positive pericentrosomal endosomes and not recruited to the plasma membrane in PC12 cells under physiological conditions. Further work will be necessary to determine whether centaurin-β2 is also recruited to the plasma membrane (or other organelles) and inactivates Arf6 in other cell types.

One remaining question is how do Rab35, centaurin-β2 and Arf6 regulate neurite outgrowth in neuronal cells. Allaire and colleagues have recently shown that knockdown of the Rab35-GEF connecdenn (DENND1A) impairs endocytic recycling of major histocompatibility complex (MHC) class I in COS-7 cells, indicating that activation of Rab35 is required for the endocytic recycling pathway to proceed (Allaire et al., 2010). Moreover, inactivation of Arf6 has been reported to be involved in the same process (Brown et al., 2001). These observations, together with a recent finding that endocytic recycling is one of the major membrane trafficking events, by which membranes and/or proteins are supplied to neurite tips during neurite outgrowth (Shirane and Nakayama, 2006; Sann et al., 2009), indicate that Rab35, centaurin-β2 and Arf6 are likely to regulate neurite outgrowth by modulating endocytic recycling. Further work will be necessary to identify the cargo, such as specific membranes and/or proteins, of the endocytic recycling pathway that is regulated by Rab35, centaurin-β2 and Arf6.

Interestingly, Rab35 and Arf6 have independently been reported to regulate other cellular events in addition to neurite outgrowth, including phagocytosis and cytokinesis (Zhang et al., 1998; Brown et al., 2001; Schweitzer and D'Souza-Schorey, 2005; Kouranti et al., 2006; Sato et al., 2008; Allaire et al., 2010; Shim et al., 2010; Dambournet et al., 2011). Because we found that Rab35, centaurin-β2 and Arf6 are ubiquitously expressed in mammalian tissues (data not shown), these previous reports, together with our own discovery of the novel crosstalk between Rab35 and Arf6 in PC12 cells, suggested that functional crosstalk between these two small GTPases through centaurin-β2 might occur in other cellular events. Very recently, while this manuscript was being prepared for publication, centaurin-β2 was reported to be involved in phagocytosis (Egami et al., 2011).

In mammals, approximately 30 Arf-GAPs, including centaurin-β2, have been predicted. We particularly took note of the fact that approximately two-thirds of Arf-GAPs contain ANKR domains (Inoue and Randazzo, 2007; Kahn et al., 2008), because the ANKR domain of several proteins, including centaurin-β2, has recently been shown to act as a specific Rab-binding domain (Johansson et al., 2007; Tamura et al., 2009; Kanno et al., 2010). One fascinating scenario is that other Arf-GAPs besides centaurin-β2 also mediate a functional crosstalk between Arf and Rab thorough their Arf-GAP domain and Rab-binding ANKR domain in a variety of cellular events. A comprehensive interaction analysis between the 60 Rab proteins and 20 Arf-GAPs in humans will be necessary to understand the full portrait of Rab- and Arf-GAP-mediated membrane trafficking in the future.

In summary, we have demonstrated by knockdown and rescue experiments that both the Rab35 effector function and Arf6-GAP activity of centaurin-β2 are essential for NGF-induced neurite outgrowth of PC12 cells. On the basis of these findings, we propose a novel concept: a Rab effector and Arf-GAP coupling mechanism (Fig. 7), in which Arf-GAP is recruited to a specific membrane compartment by its Rab effector function, by a direct interaction with specific Rab, where it then inactivates Arf in the membrane compartment.

Materials and Methods

Antibodies

Anti-Rab35 guinea pig polyclonal antibodies were produced by using purified GST-tagged mouse Rab35 (Kanno et al., 2010) (anti-GST-Rab35) and a C-terminal peptide (amino acid residues 161–180; FNCITELVLRAKKDNLAKQQ) of mouse Rab35 (anti-Rab35-C) as antigens. The anti-GST-Rab35 antibody was affinity-purified as described previously (Fukuda and Mikoshiba, 1999) and used for immunoblotting analyses. The anti-Rab35-C serum was used for immunofluorescence analyses. Anti-centaurin-β2 rabbit polyclonal antibody and anti-Rab7 rabbit polyclonal antibody were produced by using purified GST-tagged mouse centaurin-β2(ANKR) (amino acid residues 580–770) and GST-tagged mouse Rab7, respectively, as the antigen, and they were affinity-purified as described previously (Fukuda and Mikoshiba, 1999). Anti-actin goat polyclonal antibody, anti-Arf6 mouse monoclonal antibody (Santa Cruz Biotechnology, Santa Cruz, CA), anti-GM130 mouse monoclonal antibody, anti-EEA-1 mouse monoclonal antibody (BD Biosciences, San Jose, CA), anti-Rab11 rabbit polyclonal antibody (Invitrogen, Carlsbad, CA), anti-GFP rabbit polyclonal antibody (MBL, Nagoya, Japan), anti-γ-tubulin mouse monoclonal antibody, and anti-Myc rabbit polyclonal antibody (Sigma, St Louis, MO) were obtained commercially. Alexa-Fluor-488- and Alexa-Fluor-594-conjugated secondary antibodies were from Invitrogen.

RNA interference

Double-strand RNAs (siRNAs) targeting rat *Rab35* (siRab35 #1, Rab35-RSS305654 and siRab35 #2, Rab35-RSS353202) and rat *Arf6* (siArf6 #1, Arf6-RSS372677 and siArf6 #2, Arf6-RSS372678) were purchased from Invitrogen. An siRNA targeting rat *Centb2* (siCentβ2, 19-base target site: 5′-GGGTATCTGTTCAAACGAG-3′) was synthesized by Nippon EGT (Toyama, Japan). Short hairpin RNAs (shRNAs) targeting rat *Centb2* (shCentβ2 #1, 19-base target site: 5′-GGGTATCTGTTCAAACGAG-3′ and shCentβ2 #2, 19-base target site: 5′-AGACAGGAGAAGGAGGCAT-3′), mouse *Rab35* (shmsRab35 #1, 19-base target site: 5′-TATTAGTGGGCAATAAGAA-3′ and shmsRab35 #2, 19-base target site: 5′-CCAGAACTGTGACGATGTG-3′), and mouse *Centb2* (shmsCentβ2 #1, 19-base target site: 5′-AGACAGGAGAAGGAGGCAT-3′ and shmsCentβ2 #2, 19-base target site: 5′-GGGTATCTGTTCAAACGAG-3′) were constructed as described previously (Kuroda and Fukuda, 2004), using pSilencer-neo 2.0-U6 vector (Ambion, Austin, TX), which expresses shRNA. Unless otherwise stated, siRab35, siArf6, and shCentβ2 refer to siRab35 #1, siArf6 #2 and shCentβ2 #1, respectively, throughout this paper. The knockdown by each siRNA and shRNA was confirmed by its expression in PC12 cells or Neuro2a cells for 60–84 hours followed by immunoblotting with specific antibodies as described below.

Plasmids

cDNA encoding mouse Rab35(Q67L) (constitutive active mutant) was prepared as described previously (Kanno et al., 2010) and inserted into the pEGFP-C1 vector (BD Biosciences Clontech). cDNAs encoding mouse centaurin-β2, centaurin-β2(R442Q) (i.e. Arf6-GAP-activity-deficient mutant) and centaurin-β2(ΔANKR) (Rab35-binding-activity-deficient mutant) were prepared as described previously (Kanno et al., 2010). shRNA-resistant (SR) centaurin-β2 mutants [centaurin-β2^{SR}, centaurin-β2(R442Q)^{SR} and centaurin-β2(ΔANKR)^{SR}] were produced by the PCR sewing technique as follows. N-terminal-mutated fragment and C-terminal-mutated fragments were separately amplified by conventional PCR by using pEGFP-C1-centaurin-β2, pEGFP-C1-centaurin-β2(R442Q) or pEGFP-C1-centaurin-β2(ΔANKR) as a template

and the following two pairs of oligonucleotides: 5′-CATGGTCCTGCTGGAGT-3′ (pEGFP-C1-5′ primer) and 5′-GCTGGCACGCTTAAATAGGTATCCCTCCAT-3′ (mutagenic centaurin-β2^{SR} reverse primer) for the N-terminal fragment of centaurin-β2^{SR}; and 5′-ATGGAGGGATACCTATTTAAGCGTGCCAGC-3′ (mutagenic centaurin-β2^{SR} forward primer) and 5′-TTATGTTTCAGGTTCAGGGG-3′ (pEGFP-C1-3′ primer) for the C-terminal fragment. The two fragments obtained were then sewn together by PCR by using the two fragments as a mixed template and the pEGFP-C1-5′/3′ primers. The resulting centaurin-β2^{SR} fragment was inserted into the pEGFP-C1 vector and pMyc vector, which was produced by replacing the EGFP-coding sequence of pEGFP-N1 (BD Biosciences Clontech, Mountain View, CA) with a Myc-tag-coding sequence for expression of N-terminal Myc-tagged proteins. cDNA encoding mouse Arf6 was prepared as described previously (Kanno et al., 2010). Arf6(Q67L) (constitutive active mutant) was generated by the same PCR sewing technique by using pGEM-T-Arf6 as a template and the following two pairs of oligonucleotides: 5′-TAATACGACTCACTATAGGGCGA-3′ (pGEM-T-5′ primer, i.e. T7 primer) and 5′-GATCTTGTCCAGGCCGCCCAC-3′ (mutagenic Arf6-Q67L reverse primer) for the N-terminal fragment of Arf6(Q67L), and 5′-GTGGGCGGCCTGGACAAGATC-3′ (mutagenic Arf6-Q67L forward primer) and 5′-ATTTAGGTGACACTATAGAATAC-3′ (pGEM-T-3′ primer, i.e. SP6 primer) for the C-terminal fragment of Arf6(Q67L). The resulting mutated fragment was inserted into the pmStrawberry-N1 (pmStr-N1) vector, which was modified from pEGFP-N1 (BD Biosciences Clontech) by replacing the EGFP-coding sequence with an mStr-coding sequence. We performed DNA sequencing to confirm that no unexpected mutations had occurred in the open reading frame of the cDNAs described above.

Cell cultures and transfections

PC12 cells were cultured at 37℃ in Dulbecco's modified Eagle's medium (DMEM) (Sigma or Wako Pure Chemical Industries, Osaka, Japan) supplemented with 10% fetal bovine serum, 10% horse serum, 100 U/ml penicillin G and 100 μg/ml streptomycin, under 5% CO_2 (Fukuda et al., 2002). COS-7 cells and Neuro2a cells were cultured at 37℃ in DMEM supplemented with 10% fetal bovine serum, 100 U/ml penicillin G, and 100 μg/ml streptomycin, under 5% CO_2. Mouse hippocampal neurons were prepared essentially as described previously (Furutani et al., 2007). In brief, hippocampi were dissected from embryonic day 16.5 mice and dissociated with 0.25% trypsin (Invitrogen). The cells were plated at a density of 3–6 × 10^4 cells onto coverglasses in a six-well plate coated with poly-L-lysine hydrobromide (Nacalai Tesque, Kyoto, Japan). They were maintained in MEM containing B27 supplements, 1% fetal bovine serum and 0.5 mM glutamine (Invitrogen). Plasmids and/or siRNAs were transfected into cultured cells 0.5 day after plating for primary neurons and 1 day after plating for other cell cultures by using Lipofectamine Plus, Lipofectamine 2000 or Lipofectamine RNAiMAX (Invitrogen), each according to the manufacturer's instructions. To induce differentiation of PC12 cells, cells were treated with 100 ng/ml β-nerve growth factor (NGF; Merck Biosciences, Darmstadt, Germany) for the times indicated in each figure.

Immunoblotting

PC12 cells, COS-7 cells and Neuro2a cells were harvested and homogenized as described previously (Fukuda and Kanno, 2005). Total cell lysates were analyzed by 10–12.5% SDS-polyacrylamide gel electrophoresis (PAGE) followed by immunoblotting with specific primary antibodies. Immunoreactive bands were visualized with appropriate HRP-conjugated secondary antibodies and detected by enhanced chemiluminescence (ECL) (Amersham Biosciences, Buckinghamshire, UK). To evaluate the shRNA resistance of each SR construct, COS-7 cells were co-transfected with the pSilencer-centaurin-β2 (#1) knockdown construct and pEGFP-C1-centaurin-β2^{SR} construct, harvested 48 hours after transfection and analyzed by immunoblotting as described above (supplementary material Fig. S5).

Immunofluorescence

For immunofluorescence analysis, PC12 cells were fixed with either 4% paraformaldehyde (PFA) for 20 minutes, ice-cold 100% methanol for 5 minutes or 10% trichloroacetic acid (TCA) for 15 minutes, and if fixed with PFA or TCA, they were permeabilized with 0.3% Triton X-100 for 2 minutes. Immunostaining was performed with specific primary antibodies, and visualization was achieved by using appropriate secondary antibodies conjugated to Alexa Fluor 488 or 594. Some immunoreactions were enhanced by using Can Get Signal (Toyobo, Osaka, Japan). The fluorescence images of the immunostained cells were captured with a confocal fluorescence microscope (Fluoview 1000; Olympus, Tokyo, Japan). For the fluorescence intensity analyses, the relative intensity of fluorescence signals on the region of interest was calculated with MetaMorph software (version 6.3r3; Molecular Devices, Sunnyvale, CA).

Neurite-outgrowth assays

For neurite-outgrowth assay of PC12 cells, 24 hours after transfection, cells were treated with NGF for 36 hours. Cells were then fixed with 4% PFA for 20 minutes, and images of the transfected cells were captured at random with a confocal microscope (n>100 from three dishes for each experiment). For neurite-outgrowth assay of primary neurons, cells at 4 days in vitro (DIV) were fixed with 4% PFA for 20 minutes. Images of the transfected cells were captured at random with a confocal microscope (n=60 from three independent experiments for each shRNA). siRNA- or shRNA-transfected cells were labeled by co-transfection with EGFP expression vector. The total length of all neurites extended from individual cells, which we refer to as total neurite length in this study, was measured with MetaMorph software. Neurite-outgrowth assays were performed at least three times for each siRNA or shRNA, or each construct. The results of the neurite outgrowth assays reported in this paper are means and standard error (s.e.) of the data from one experiment that was representative of at least three independent experiments with similar results.

Colocalization analyses

For colocalization analyses, PC12 cells were treated with NGF for 6 hours. Cells were then fixed and stained with antibodies against centaurin-β2 (or Rab35) and the organelle markers indicated in Fig. 2A, Fig. 4A and supplementary material Fig. S4A. Cells were selected at random, and two fluorescence images (Alexa-Fluor-488-labeled image and Alexa-Fluor-594-labeled image) of the cells were captured sequentially to prevent bleed-through of fluorescence under conditions in which none of the fluorescence signals was saturated (n=30 from three independent experiments for each colocalization analysis). After the background signals of each of the images had been subtracted by using the BG Subtraction from ROI plugin of ImageJ software (version 1.44o; NIH), for background correction, a 20 μm^2 area in the perinuclear regions that contained Rab35 or centaurin-β2 signals was selected as a region of interest (ROI). A Pearson's correlation coefficient (PCC) value for the relation between the Alexa-Fluor-488-labeled signals and Alexa-Fluor-594-labeled signals of the ROI then calculated with the Intensity Correlation Analysis plug-in of ImageJ software. The results of the colocalization analyses are reported as means and standard deviation (s.d.).

Quantification of the pericentrosomal signals of Rab35 and centaurin-β2

For quantification of pericentrosomal signals, 54 hours after transfection of siRab35 or siCentβ2, PC12 cells were treated with NGF for 6 hours. Cells were then fixed and stained with an antibody against Rab35 or centaurin-β2, and fluorescence images of the transfected cells were captured at random under conditions in which none of the fluorescence signals was saturated (n=30 from three independent experiments for each quantification analysis). Cytosolic signals were then subtracted from the images to obtain true pericentrosomal signals. After the subtraction, a 3 μm^2 area in the pericentrosomal region was selected as a ROI, and the relative intensities of the fluorescence signals of the ROI were measured as pericentrosomal signals of Rab35 and centaurin-β2 with MetaMorph software. Pericentrosomal regions were identified by the immunofluorescence signals of γ-tubulin, a centrosome marker. The results of quantification are reported as means and s.e. The pericentrosomal signal intensity of Rab35 or centaurin-β2 in the control cells for each experiment is expressed as 100 (arbitrary units, a.u.).

Statistical analyses

Results of the colocalization analyses are reported as means ± s.d., and the results of the neurite outgrowth assays and pericentrosomal signals as means and s.e. For evaluating significance, every result was compared with the results of control cells by using Student's unpaired t-test. *P<0.05, **P<0.01 in comparison with the control cells.

Acknowledgements

We thank Megumi Aizawa for technical assistance, Yasunori Mori for preparing mouse hippocampal neurons, and members of the Fukuda Laboratory for valuable discussions.

Funding

This work was supported in part by Grants-in-Aid for Scientific Research from the Ministry of Education, Culture, Sports, and Technology (MEXT) of Japan (to M.F.) and by a grant from the Global COE Program (Basic & Translational Research Center for Global Brain Science) of the MEXT of Japan (to M.F.). H.K. was supported by the Japan Society for the Promotion of Science (JSPS) and by the International Advanced Research and Education Organization of Tohoku University (IAREO).

Supplementary material available online at
http://jcs.biologists.org/lookup/suppl/doi:10.1242/jcs.098657/-/DC1

References

Albertinazzi, C., Za, L., Paris, S. and de Curtis, I. (2003). ADP-ribosylation factor 6 and a functional PIX/p95-APP1 complex are required for Rac1B-mediated neurite outgrowth. *Mol. Biol. Cell* **14**, 1295-1307.

Allaire, P. D., Marat, A. L., Dall'Armi, C., Di Paolo, G., McPherson, P. S. and Ritter, B. (2010). The Connecdenn DENN domain: a GEF for Rab35 mediating cargo-specific exit from early endosomes. *Mol. Cell* **37**, 370-382.

Barr, F. and Lambright, D. G. (2010). Rab GEFs and GAPs. *Curr. Opin. Cell Biol.* **22**, 461-470.

Brown, F. D., Rozelle, A. L., Yin, H. L., Balla, T. and Donaldson, J. G. (2001). Phosphatidylinositol 4,5-bisphosphate and Arf6-regulated membrane traffic. *J. Cell Biol.* **154**, 1007-1017.

Chevallier, J., Koop, C., Srivastava, A., Petrie, R. J., Lamarche-Vane, N. and Presley, J. F. (2009). Rab35 regulates neurite outgrowth and cell shape. *FEBS Lett.* **583**, 1096-1101.

Dambournet, D., Machicoane, M., Chesneau, L., Sachse, M., Rocancourt, M., El Marjou, A., Formstecher, E., Salomon, R., Goud, B. and Echard, A. (2011). Rab35 GTPase and OCRL phosphatase remodel lipids and F-actin for successful cytokinesis. *Nat. Cell Biol.* **13**, 981-988.

Donaldson, J. G. (2003). Multiple roles for Arf6: sorting, structuring, and signaling at the plasma membrane. *J. Biol. Chem.* **278**, 41573-41576.

D'Souza-Schorey, C. and Chavrier, P. (2006). ARF proteins: roles in membrane traffic and beyond. *Nat. Rev. Mol. Cell Biol.* **7**, 347-358.

Egami, Y., Fukuda, M. and Araki, N. (2011). Rab35 regulates phagosome formation through recruitment of ACAP2 in macrophages during FcγR-mediated phagocytosis. *J. Cell Sci.* **124**, 3557-3567.

Fielding, A. B., Schonteich, E., Matheson, J., Wilson, G., Yu, X., Hickson, G. R., Srivastava, S., Baldwin, S. A., Prekeris, R. and Gould, G. W. (2005). Rab11-FIP3 and FIP4 interact with Arf6 and the exocyst to control membrane traffic in cytokinesis. *EMBO J.* **24**, 3389-3399.

Fukuda, M. (2008). Regulation of secretory vesicle traffic by Rab small GTPases. *Cell. Mol. Life Sci.* **65**, 2801-2813.

Fukuda, M. and Kanno, E. (2005). Analysis of the role of Rab27 effector Slp4-a/granuphilin-a in dense-core vesicle exocytosis. *Methods Enzymol.* **403**, 445-457.

Fukuda, M. and Mikoshiba, K. (1999). A novel alternatively spliced variant of synaptotagmin VI lacking a transmembrane domain: implications for distinct functions of the two isoforms. *J. Biol. Chem.* **274**, 31428-31434.

Fukuda, M., Kanno, E., Saegusa, C., Ogata, Y. and Kuroda, T. S. (2002). Slp4-a/granuphilin-a regulates dense-core vesicle exocytosis in PC12 cells. *J. Biol. Chem.* **277**, 39673-39678.

Fukuda, M., Kanno, E., Ishibashi, K. and Itoh, T. (2008). Large scale screening for novel rab effectors reveals unexpected broad Rab binding specificity. *Mol. Cell. Proteomics* **7**, 1031-1042.

Fukuda, M., Kobayashi, H., Ishibashi, K. and Ohbayashi, N. (2011). Genome-wide investigation of the Rab binding activity of RUN domains: development of a novel tool that specifically traps GTP-Rab35. *Cell Struct. Funct.* **36**, 155-170.

Furutani, Y., Matsuno, H., Kawasaki, M., Sasaki, T., Mori, K. and Yoshihara, Y. (2007). Interaction between telencephalin and ERM family proteins mediates dendritic filopodia formation. *J. Neurosci.* **27**, 8866-8876.

Hernández-Deviez, D. J., Roth, M. G., Casanova, J. E. and Wilson, J. M. (2004). ARNO and ARF6 regulate axonal elongation and branching through downstream activation of phosphatidylinositol 4-phosphate 5-kinase α. *Mol. Biol. Cell* **15**, 111-120.

Hsu, C., Morohashi, Y., Yoshimura, S., Manrique-Hoyos, N., Jung, S., Lauterbach, M. A., Bakhti, M., Grønborg, M., Möbius, W., Rhee, J. et al. (2010). Regulation of exosome secretion by Rab35 and its GTPase-activating proteins TBC1D10A-C. *J. Cell Biol.* **189**, 223-232.

Inoue, H. and Randazzo, P. A. (2007). Arf GAPs and their interacting proteins. *Traffic* **8**, 1465-1475.

Jackson, T. R., Brown, F. D., Nie, Z., Miura, K., Foroni, L., Sun, J., Hsu, V. W., Donaldson, J. G. and Randazzo, P. A. (2000). ACAPs are arf6 GTPase-activating proteins that function in the cell periphery. *J. Cell Biol.* **151**, 627-638.

Jaworski, J. (2007). ARF6 in the nervous system. *Eur. J. Cell Biol.* **86**, 513-524.

Johansson, M., Rocha, N., Zwart, W., Jordens, I., Janssen, L., Kuijl, C., Olkkonen, V. M. and Neefjes, J. (2007). Activation of endosomal dynein motors by stepwise assembly of Rab7-RILP-p150^{Glued}, ORP1L, and the receptor βIII spectrin. *J. Cell Biol.* **176**, 459-471.

Kahn, R. A., Bruford, E., Inoue, H., Logsdon, J. M., Jr, Nie, Z., Premont, R. T., Randazzo, P. A., Satake, M., Theibert, A. B., Zapp, M. L. et al. (2008). Consensus nomenclature for the human ArfGAP domain-containing proteins. *J. Cell Biol.* **182**, 1039-1044.

Kanno, E., Ishibashi, K., Kobayashi, H., Matsui, T., Ohbayashi, N. and Fukuda, M. (2010). Comprehensive screening for novel rab-binding proteins by GST pull-down assay using 60 different mammalian Rabs. *Traffic* **11**, 491-507.

Kouranti, I., Sachse, M., Arouche, N., Goud, B. and Echard, A. (2006). Rab35 regulates an endocytic recycling pathway essential for the terminal steps of cytokinesis. *Curr. Biol.* **16**, 1719-1725.

Kuroda, T. S. and Fukuda, M. (2004). Rab27A-binding protein Slp2-a is required for peripheral melanosome distribution and elongated cell shape in melanocytes. *Nat. Cell Biol.* **6**, 1195-1203.

Lin, S. X., Grant, B., Hirsh, D. and Maxfield, F. R. (2001). Rme-1 regulates the distribution and function of the endocytic recycling compartment in mammalian cells. *Nat. Cell Biol.* **3**, 567-572.

Patino-Lopez, G., Dong, X., Ben-Aissa, K., Bernot, K. M., Itoh, T., Fukuda, M., Kruhlak, M. J., Samelson, L. E. and Shaw, S. (2008). Rab35 and its GAP EPI64C in T cells regulate receptor recycling and immunological synapse formation. *J. Biol. Chem.* **283**, 18323-18330.

Sann, S., Wang, Z., Brown, H. and Jin, Y. (2009). Roles of endosomal trafficking in neurite outgrowth and guidance. *Trends Cell Biol.* **19**, 317-324.

Sato, M., Sato, K., Liou, W., Pant, S., Harada, A. and Grant, B. D. (2008). Regulation of endocytic recycling by *C. elegans* Rab35 and its regulator RME-4, a coated-pit protein. *EMBO J.* **27**, 1183-1196.

Schonteich, E., Pilli, M., Simon, G. C., Matern, H. T., Junutula, J. R., Sentz, D., Holmes, R. K. and Prekeris, R. (2007). Molecular characterization of Rab11-FIP3 binding to ARF GTPases. *Eur. J. Cell Biol.* **86**, 417-431.

Schweitzer, J. K. and D'Souza-Schorey, C. (2005). A requirement for ARF6 during the completion of cytokinesis. *Exp. Cell Res.* **311**, 74-83.

Shiba, T., Koga, H., Shin, H. W., Kawasaki, M., Kato, R., Nakayama, K. and Wakatsuki, S. (2006). Structural basis for Rab11-dependent membrane recruitment of a family of Rab11-interacting protein 3 (FIP3)/Arfophilin-1. *Proc. Natl. Acad. Sci. USA* **103**, 15416-15421.

Shim, J., Lee, S. M., Lee, M. S., Yoon, J., Kweon, H. S. and Kim, Y. J. (2010). Rab35 mediates transport of Cdc42 and Rac1 to the plasma membrane during phagocytosis. *Mol. Cell. Biol.* **30**, 1421-1433.

Shirane, M. and Nakayama, K. I. (2006). Protrudin induces neurite formation by directional membrane trafficking. *Science* **314**, 818-821.

Stenmark, H. (2009). Rab GTPases as coordinators of vesicle traffic. *Nat. Rev. Mol. Cell Biol.* **10**, 513-525.

Tamura, K., Ohbayashi, N., Maruta, Y., Kanno, E., Itoh, T. and Fukuda, M. (2009). Varp is a novel Rab32/38-binding protein that regulates Tyrp1 trafficking in melanocytes. *Mol. Biol. Cell* **20**, 2900-2908.

van Ijzendoorn, S. C. D. (2006). Recycling endosomes. *J. Cell Sci.* **119**, 1679-1681.

Wennerberg, K., Rossman, K. L. and Der, C. J. (2005). The Ras superfamily at a glance. *J. Cell Sci.* **118**, 843-846.

Yamauchi, J., Miyamoto, Y., Torii, T., Mizutani, R., Nakamura, K., Sanbe, A., Koide, H., Kusakawa, S. and Tanoue, A. (2009). Valproic acid-inducible Arl4D and cytohesin-2/ARNO, acting through the downstream Arf6, regulate neurite outgrowth in N1E-115 cells. *Exp. Cell Res.* **315**, 2043-2052.

Zerial, M. and McBride, H. (2001). Rab proteins as membrane organizers. *Nat. Rev. Mol. Cell Biol.* **2**, 107-117.

Zhang, J., Fonovic, M., Suyama, K., Bogyo, M. and Scott, M. P. (2009). Rab35 controls actin bundling by recruiting fascin as an effector protein. *Science* **325**, 1250-1254.

Zhang, Q., Cox, D., Tseng, C. C., Donaldson, J. G. and Greenberg, S. (1998). A requirement for ARF6 in Fcgamma receptor-mediated phagocytosis in macrophages. *J. Biol. Chem.* **273**, 19977-19981.